ISSN 0915-633X

INTERNATIONAL ATOMIC ENERGY AGENCY

18th IAEA Fusion Energy Conference
Sorrento, Italy, 4 to 10 October 2000

IAEA-CN-77/ EX9/1

NATIONAL INSTITUTE FOR FUSION SCIENCE

Study of Energetic Ion Transport in the Large Helical Device

M. Sasao, S. Murakami, M. Isobe; A.V. Krasilnikov, S. Iiduka, K. Itoh, N. Nakajima, M. Osakabe, K.Saito,T. Seki, Y.Takeiri, T. Watari, N.Ashikawa , P.deVaries, M.Emoto, H.Funaba, M.Goto, K.Ida, H.Idei, K.Ikeda, S.Inagaki, N:Inoue, S.Kado, O.Kaneko, K.Kawahata, K.Khlopenkov, T.Kobuchi , A.Komori, S.Kubo, R.Kumazawa, S.Masuzaki, T.Minami, J.Miyazawa, T.Morisaki, S.Morita, S.Muto, T.Mutoh, Y.Nagayama, Y.Nakamura, H:Nakanishi, K.Narihara, K.Nishimura, N.Noda, T.Notake, Y.Liang , S.Ohdachi, N.Ohyabu, Y.Oka, T.Ozaki, R.O.Pavlichenko, B.J.Peterson, A.Sagara, S.Sakakibara, R.Sakamoto, H.Sasao, K.Sato, M.Sato, T.Shimozuma, M.Shoji, H.Suzuki, M.Takechi, N.Tamura, K.Tanaka, K.Toi, T.Tokuzawa, Y.Torii, K.Tsumori, H.Yamada, I.Yamada, S.Yamaguchi, S.Yamamoto, M.Yokoyama, Y.Yoshimura, K.Y.Watanabe and O. Motojima

(Received - Sep. 14, 2000)

NIFS-657 Sep. 2000

RESEARCH REPORT
NIFS Series

TOKI, JAPAN

Study of Energetic Ion Transport in the Large Helical Device

M. Sasao 1), S. Murakami 1), M. Isobe 1), A.V. Krasilnikov 2), S. Iiduka 3), K. Itoh 1), N. Nakajima 1), M. Osakabe 1), K.Saito 4),T. Seki 1), Y.Takeiri 1), T. Watari 1), H.Yamada 1), N.Ashikawa 5), P.deVaries 1), M.Emoto 1), H.Funaba 1), M.Goto 1), K.Ida, 1) H.Idei 1), K.Ikeda 1), S.Inagaki 1), N.Inoue 1), S.Kado 1), O.Kaneko 1), K.Kawahata 1), K.Khlopenkov 1), T.Kobuchi 5), A.Komori 1), S.Kubo 1), R.Kumazawa 1), S.Masuzaki 1), T.Minami 1), J.Miyazawa 1), T.Morisaki 1), S.Morita 1), S.Muto 1), T.Mutoh 1), Y.Nagayama 1), Y.Nakamura 1), H.Nakanishi 1), K.Narihara 1), K.Nishimura 1), N.Noda 1), T.Notake 4,) Y.Liang 5), S.Ohdachi 1), N.Ohyabu 1), Y.Oka 1), T.Ozaki 1), B.J.Peterson 1), R.O.Pavlichenko 1), A.Sagara 1), S.Sakakibara 1), R.Sakamoto 1), H.Sasao 5), K.Sato 1), M.Sato 1), T.Shimozuma 1), M.Shoji 1), H.Suzuki 1), M.Takechi 1), N.Tamura 5), K.Tanaka 1), K.Toi 1), T.Tokuzawa 1), Y.Torii 4), K.Tsumori 1), , I.Yamada 1), S.Yamaguchi 1), S.Yamamoto 4), M.Yokoyama 1), Y.Yoshimura 1), K.Y.Watanabe 1), O. Motojima 1), and M. Fujiwara 1)

1)National Institute for Fusion Science, Toki, 509-5292, Japan
2)Troitsk Institute for Innovating and Fusion Research, Troitsk, Russia
3) Department of Nuclear Engineering, Nagoya University, 464-8603, Japan
4) Department of Energy Engineering and Science, Nagoya University, 464-8603, Japan
5) Department of Fusion Science, School of Mathematical and Physical Science, Graduate University for Advanced Studies, Hayama, 240-0193, Japan

E-mail: sasao@nifs.ac.jp

Abstract: The confinement property of high energy ions and the role of ripple induced transport have been studied in the Large Helical Device (LHD). Tangential beam particles are injected at 90 - 150 kV by negative-ion-based neutral beam injectors, and perpendicular high energy particles are generated by Ion Cyclotron Range of Frequency (ICRF) heating. Energy distributions of high energy ions have been measured by fast neutral particle analyzers based on natural diamond detectors, specially developed for this experiment. Time evolution of perpendicular tail temperature in decaying phase after the ICRF termination indicates that the fast particles deeply trapped in helical ripples are well confined longer than the collisional relaxation time, when $n_e > 10^{19}$ m^{-3} in the inward shifted configuration (R_{ax} = 3.6 m). In lower density plasma, however, faster decay than the classical prediction is observed. The tangential energy spectra in a low density steady state plasma of the standard configuration (R_{ax} = 3.75 m) also show the deviation from 2D Fokker-Plank simulation. The global 5-D transport simulation code including the ripple induced transport shows good agreement with measured spectra, and this suggests an important role of ripple induced transport in the standard configuration of LHD.

1. Introduction

The energetic ion behavior in helical systems is of great interest from view points of difference of the symmetry in the magnetic configuration from that of tokamaks, and hence difference in ripple and loss cone structures. The confinement of energetic ions is also one of key issues for the prospect to a steady state reactor plasma using a helical system[1]. Complex motions of trapped particles in helical systems tend to enhance the radial transport. There are extensive theoretical works on the particle orbits in helical systems[2,3], but not so much works on the effect of ripple induced transport are accumulated. Several experimental works have been done in Advanced Toroidal Facility[4], Wendelstein 7-AS[5], Heliotron-E[6], and Compact Helical System[7-9], by observing fast neutral particles, neutron fluxs, and the global change of plasma parameters and plasma pressure. In Heliotron-E, the tail formation by ICRF is extensively studied and the fast decay after termination of the ICRF shows the

importance of the orbit loss in helical systems.

In the present work, behaviors of high energy ions injected tangentially by neutral beam injectors and those of perpendicular particles produce by ICRF heating in the Large Helical Device are investigated by observing fast neutral particles tangentially and radially. The formation of the high energy tail and its time evolution are studied in wide range of collisionality parameter. The theoretical calculations using the global 5-D simulation code including the ripple induced transport have been performed, and the tangential energy spectra in steady state beam heated plasma are compared with simulation results.

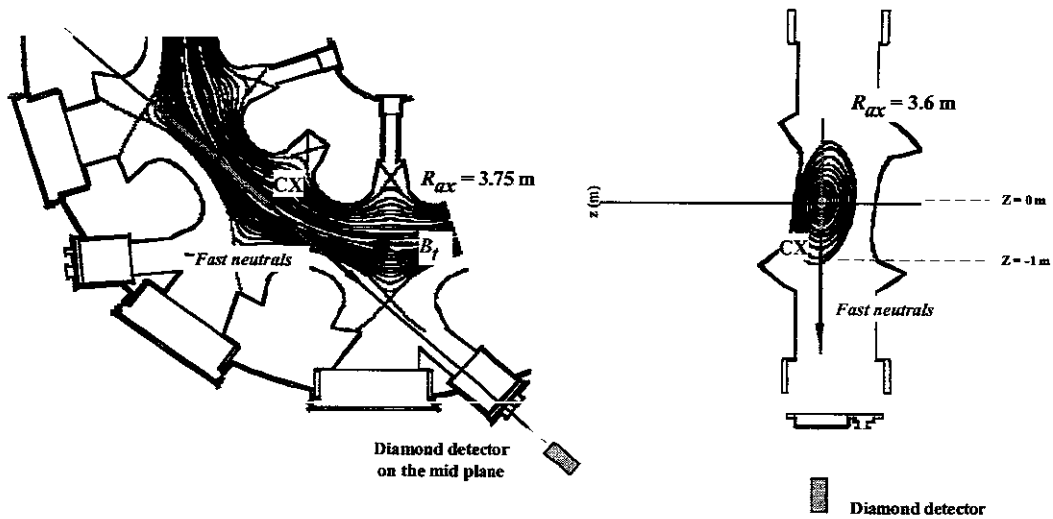

Fig. 1 Experimental set-up for the high energy particle studies in LHD, showing (a) the tangential viewing line and (b) the perpendicular line of the Diamond-NPA's.

2. Experimental Set-up and Energetic Particle Orbits in LHD

The LHD is an l=2/m=10 heliotron type device with superconducting helical and poloidal coils[10]. In the present experiment, the major radius of the magnetic axis (R_{ax}), the averaged minor radius (a), and the magnetic field strength at the axis (B_t) are 3.75 m, 0.6 m, 1.5 T for NBI experiment, and 3.6 m, 0.6 m, 2.75 T for ICRF heating experiment, respectively. In LHD the magnetic configuration of R_{ax} = 3.75 m is standard and considered to be well-ballanced from the points for MHD stability and particle confinement, but that of inward shifted (R_{ax} =3.6 m) is expected to have better trapped particle confinement, because the mod-B minimum contours are close to magnetic flux surfaces[11,12]. The plasma is initially produced by 0.4 MW ECRH (82.6 GHz, 84 GHz) and it is heated by ICRF and/or by two neutral beams, which are injected tangentially in co- and/or ctr-direction with the energy up to 150 keV and with total power up to 4 MW. The ICRF wave is injected into helium plasma with hydrogen minority from the outer side antenna of the vertically elongated poloidal section, with power up to 1.5 MW at frequency 38.46 MHz[12,13,14].

Two sets of fast charge exchange atom spectrometers based on natural diamond detector (Diamond-NPA) are developed and used for confined fast ion spectrometry[15,16], one with vertical and the other tangential line of sight. In figure 1 is shown the experimental

arrangement for the high energy particle studies in the present work; a) for the vertical and b) for tangential measurement. The vertical line of sight covers the pitch angle range(χ) of 82° ~102 °, and the tangential line of sight covers the pitch angle range of 140° ~180°.

Energetic particles in a heliotron system are sometimes categorized by their orbits into passing particles, mirror trapped particles, deeply trapped particles in the helical ripples and transitions particles[2]. The orbits of 150 keV protons starting from points at R=3.7 m in a z-χ plane are shown in Fig. 2a by various symbols. Most of tangentially injected beam particles are in the passing orbit, while the boundary of this orbit is mostly determined by its trap into the transition particle orbit, which shows a complex behavior, due to reflection by various kind of ripples. Deeply trapped particles, the banana centers of which move poloidally and toroidally along the minimum B of the helical ripple, are distributed in the outer region of an R-χ plane. In figure 2b is shown the poloidal cross section of magnetic closed surfaces, together with the cyclotron resonance surfaces for H^- minority ions in the present experimental regime, which are placed in upper and lower parts of the plasma cross section. The perpendicular particle orbits of 150 keV protons starting various locations in this plane are shown here by same symbols. The perpendicular particles near the cyclotron resonance surfaces are mostly deeply trapped in the helical ripples, and particles of the viewing line of vertical NDD are also deeply trapped. The transition particles are distributed at the boundary of deeply trapped orbit. Tangentially injected beam particles are diffused in a $v_{//}$-$v_\perp$ space, crossing the unstable transition orbit region. During synergic heating phase of the ICRF application to NBI-heated plasma, beam particles are accelerated towards perpendicular direction crossing this unstable region, and finally trapped in helical ripples. The importance of present study is in diffusion of these energetic particles due to combination of collisional effect and the ripple induced complexity of particle orbits.

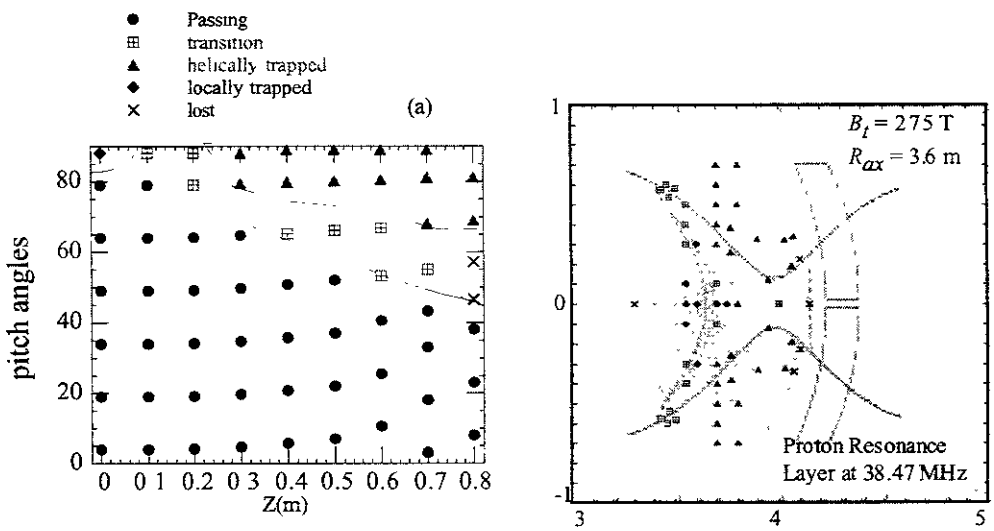

Fig. 2 (a) Distribution of particle orbits of 150keV protons in a z-χ plane at R=3.7 m for B_t=2.75T, and R_{ax} = 3.6 m. Circles represent those in passing orbit, triangles in deeply trapped orbits, rectangular's are in transition orbit and crosses are in prompt loss region. (b) The poloidal cross section of magnetic closed surfaces toghther with the cyclotron resonance surfaces for H^+ minority ions and symbols for perpendicular particle orbits.

3. Experimental results

In order to derive proton spectrum confined in plasma from measured neutral counts, hydrogen neutrals (H^0) in a hydrogen plasma or He^0/ He^+ 's in a helium plasma are

responsible for neutralization of high energy particles. A code for neutral distribution using a simplified model has been developed to calculate both H^0 and He^0 distribution, and used in the present analysis. The H^0/He^0 penetration strongly depends on its speed crossing the last closed magnetic flux surface (LCFS). In LHD the neutral temperature at LCFS is thought to be about several eV, and its density is in the order of 10^{-3} of the central plasma density. The H^0/He^0 penetration depends also on the plasma density. As the density increased, the central H^0 or He^0 density becomes less. Inside the plasma, hydrogen atoms are reproduced through the single charge exchange process while helium neutrals are produced through the double charge exchange process. On the other hand, the He^+ density is mostly determined by the ratio of the electron impact ionization rate and recombination rate, and linearly increased with the plasma density but strongly decreased with T_e.

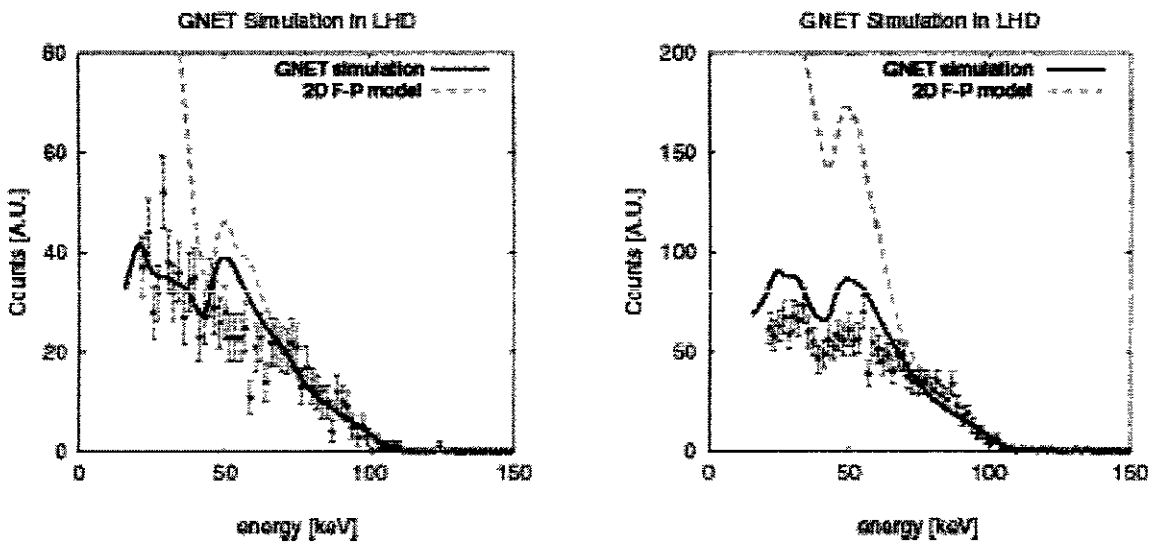

Fig. 3. The NDD pulse height spectra with error bars for two different densities in the LHD; 1.5 x 10^{19} m^{-3} (left) and 0.7 x 10^{19} m^{-3} (right). Dashed and solid lines show the predictions by 2D Fokker-Planck calculation and the simulated NDD count number using the GNET results, respectively.

3.1 Energy Spectra of Tangential viewing line

Figure 3 shows the counting spectra number measured by the tangenail Diamond-NPA, before the charge exchange correction, for two different time periods of a NBI-heated discharge hydrogen. The the total beam power of co/ctr- injecttion is 1.1 MW, and the electron temperature is ranging in 1-2 keV. In this discharge (the standard configuration; R_{ax} = 3.75 m) the plasma density increases up to 1.5 x 10^{19} m^{-3} and, then, decreased to 0.7 x 10^{19} m^{-3}. The beam particle (E_b = 100keV) was tangentially injected and slows down to the thermal energy. We can see the nearly linear increase in NDD pulse height spectrum as energy decreases in the higher density case. On the other hand the saturation in the pulse height spectrum is found as energy decreases in the lower density case. The dashed lines show the prediction by 2D Fokker-Planck simulation, including the charge exchange rate due to H^0, and the particle attenuation by re-ionization in a plasma. Here no radial transport effect on beam ion is taken into account. Large differences between the experimental and 2D simulation results are seen below about 40keV. This difference is enhanced in the low density

case. The simulation considering ripple induced transport is discussed in the next chapter.

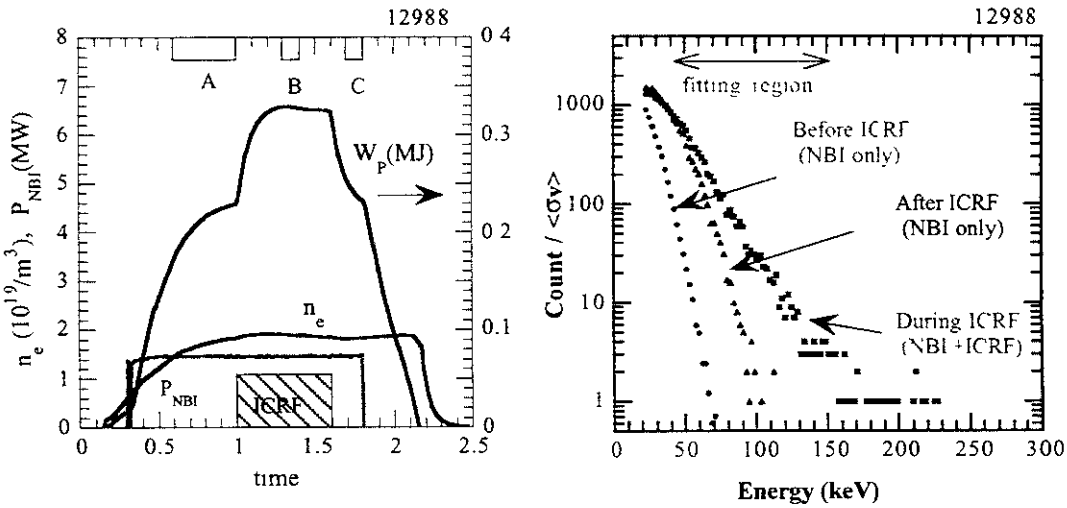

Fig 4 Time evolutions of plasma density and that of stored energy of a synergic discharge with ICRF Heating superposed on NBI target plasma(a), and perpendicular proton spectra of before (A:circles), during (B:boxes), and after(C:triangles) the ICRF heating. The absorbed ICRF power is about 1.05 MW, and the central electron temperature is 2.5 keV.

3.2 Energy spectra measured by vertical NDD and high energy tail formation by ICRF

High performance ICRF experiment was carried out with the minority heating regime in the configuration of B_t=2.75T, and R_{ax} = 3.6 m, with the ICRF self sustained scenario and the synergic heating scenario of ICRF on NBI plasma[12,13,14]. Here hydrogen is the minority in a helium plasma. Fig. 4 shows (a) time evolutions of plasma density, the stored energy and (b) energy spectra measured by the perpendicular diamond-NPA during the NBI only and the after the ICRF heating starts and after its termination. Clear change of the spectrum and the formation of the high energy tail by ICRF can be seen. Because the Diamond-NPA had counting capability up to 2 x10^5/sec, the tail temperature (T^{eff}) can be derived from the slopes of the spectra for every 10 msec. In Fig. 5 is shown the time evolution of T^{eff} for two cases, (a) at relatively low density of 1 x 10^{19} m $^{-3}$ and (b) at 2 x 10^{19} m $^{-3}$. Here the central T_e of the ICRF+NBI phase is about 2.5 keV for both cases. In most of discharges of this scenario, a clear increase of T^{eff} is observed. After the ICRF termination, the T^{eff} is gradually decreasing. The e-folding decay time of T^{eff} , i.e. the relaxation time of high energy tail, for the higher density case(b) is shorter than the decay time of the lower density case. In Fig. 6 the measured decay time, τ_m is compared with the classical Coulomb relaxation time, τ_{cl}. As the τ_{cl} is increased in the low density, high T_e region, the τ_m is going to be saturated at a level about 100 ms.

In Fig. 5 is also shown the time evolution of the integrated flux of high energy tail component. The integrated flux does not decrease after the ICRF termination, but slightly increased. This increase cannot be explained by the change of He^0 density resulting from the change of plasma parameters (n_e is constant and T_e decreases about 20 – 30 %), if we assume the He^0 is the main source of neutralization of the fast ions. However, if we assume that the He^+ is the main source of neutralization, then the increase of He^+ due to decrease of T_e can reproduce the

change of the integrated flux of fast particles. The calculated high energy neutral flux without loss are shown by solid lines. Together with the agreement of measured decay time of the tail temperature with classical prediction, present measurement indicates that deeply trapped ions are well confined until they transfer their energy to a bulk plasma when the density is higher than $1x10^{19}/m^3$. However, the T^{eff} decays faster than the classical prediction when the density is low. Charge exchange loss would be one of the reasons. The charge exchange rate $<\sigma v>$, however, has an energy dependence which has maximum at around 30 keV for He^0 , and at around 50 keV for He^+ . So the charge exchange loss cannot explain faster decay of the tail temperature. The ripple induced effect is the most probable reasons.

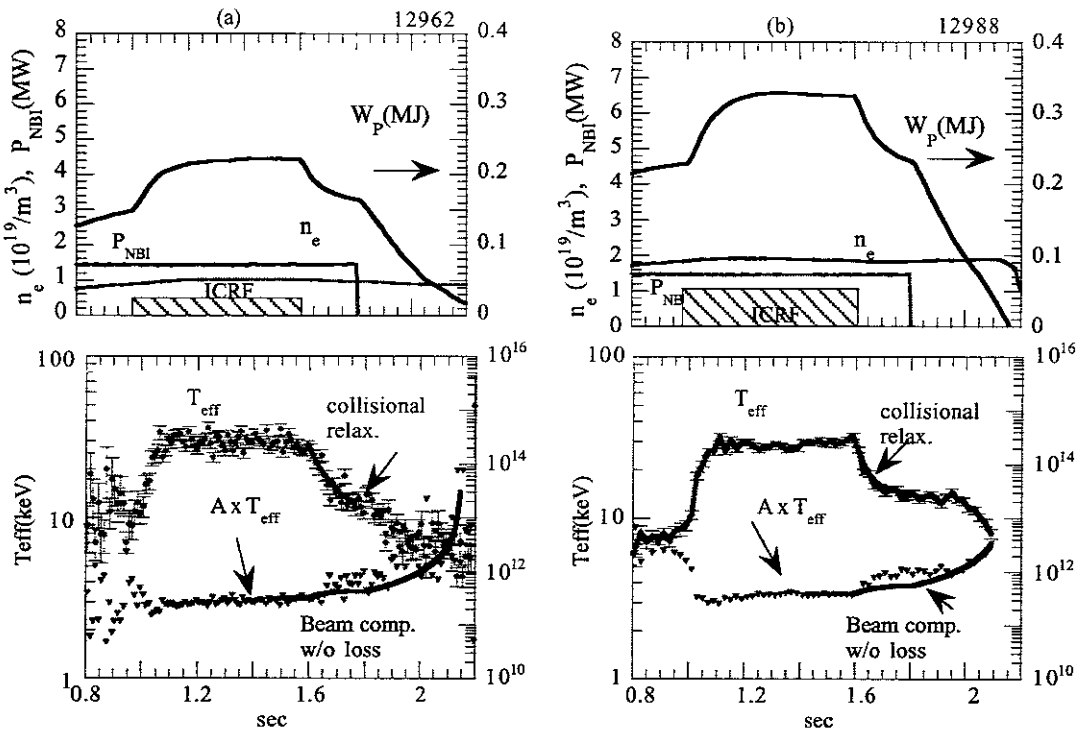

Fig. 5. Time evolutions of plasma density and that of stored energy Time evolution of T^{eff} and total integrated flux during ICRF which is imposed on a NBI heated plasma measured (B_T=2.75T, R_{ax}=3.6m). (a) discharge at relatively low density 1 x 10^{19} m^{-3} and (a) discharge at 2 x 10^{19} m^{-3} . The solid lines represent calculated high energy neutral flux without loss.

4. Ripple Induced Transport Analysis

Several explanations can also be considered for the difference in count number in tangential spectra (Fig. 3); e.g. anomalous transport, strong charge exchange effect, etc. Among them, radial transport due to the helical trapped particle is a plausible cause of this difference. To clarify this point we study the ripple induced transport of energetic ions using GNET code[17],where the drift kinetic equation in 5D phase-space is solved in the LHD plasma with The initial condition of

$$f(\mathbf{x}, v_{//}, v_{\perp}, t=0)=0$$

as

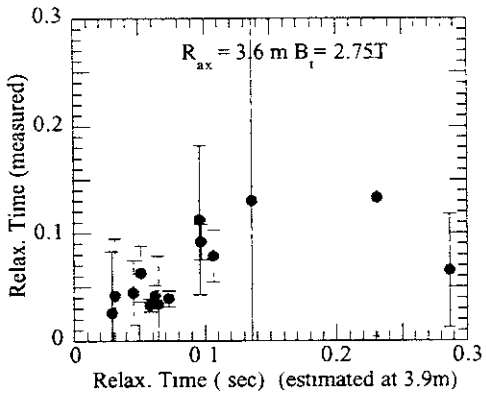

Fig.6 Comparison of the measured decay time of T^{eff} and the classical Coulomb relaxation time τ_{cl}.

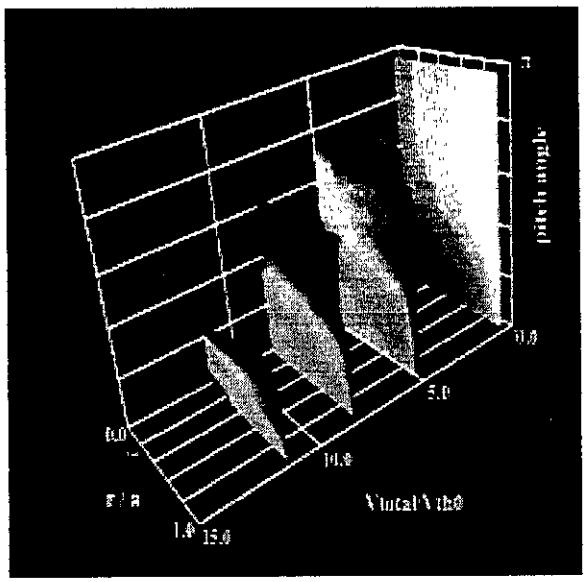

Fig 7 : Contour plots of the energetic ion distribution in the (r/a, v, θ_p/π) coordinates in the LHD plasma (lower density case).

$$\frac{\partial f}{\partial t} + (\mathbf{v}_d + \mathbf{v}_{ll}) \cdot \frac{\partial f}{\partial \mathbf{x}} + \dot{\mathbf{v}} \cdot \frac{\partial f}{\partial \mathbf{v}} - C^{col}(f) = S^{NBI}(\mathbf{x}, v_{ll}, v_{\perp})$$

where C^{Col} is the collision operator and S^{NBI} is the heating source term for NBI heating, which is evaluated by HFREYA code[18]. Figure 7 shows the steady state distribution with the NBI beam source obtained by GNET code in the three dimensional space (r/a, v, θ_p/π), where r/a , v, and θ_p are the averaged minor radius, the total velocity and the pitch angle, respectively. The NBI heating and plasma parameters are assumed based on the parameters of the lower density case in Fig. 3. The beam ions deposit at the high velocity region ($v \sim 11\ v_{th0}$) and slow down to the thermal velocity. When the beam ion reaches to the critical velocity (about 5 times of thermal velocity), the pitch angle scattering takes place via the collisions with background ions, and the beam ion distribution spreads toward the higher pitch angle region (upper side in Fig.7). We can see the decrease of the distribution due to the ripple induced diffusion at the radial region, r/a > 0.6, where the fraction of trapped particle becomes large. We can see the deficit of distribution in the trapped particle region near the edge region caused by the direct convective transport of trapped particle to the outside of plasma. As is shown in Fig. 3, the decrease of the distribution is clearer in the lower density case (right) compared with that of the higher density case (left) because of lower collisionality,. These results indicate the significant role of the ripple induced transport in the energetic ion confinement in the LHD. Using the obtained distribution by GNET code we have evaluated the neutral particle number detected by Diamond-NPA (Fig. 3). The clear decrease of count number due to the ripple induced transport from the 2D F-P results is reproduced in both density cases. Also the larger decrease due to the larger ripple induced transport is obtained in the lower density case. Consequently, we obtain good agreement in both density cases and this indicates the role of ripple induced transport in the radial transport process in the LHD.

5. Conclusion

Confinement property of energetic ions in LHD can be summarized as the following. Both passing and deeply trapped particles are well confined so that they slow down classically and significant orbit losses are not observed, when $n_e > 10^{19}$ m^{-3} in the inward shifted configuration (R_{ax} = 3.6 m). In a low collisionality plasma, however, deviation from the classical prediction is observed, especially in the standard configuration (R_{ax} = 3.75 m), indicating the ripple induced effect. The global 5-D simulation code including the ripple induced transport shows good agreement with the measured fast neutral spectra and this suggests an important role of ripple induced transport in the standard configuration of LHD.

The authors would like to thank Dr. D.S. Darrow for his development of orbit calculation code for LHD and for useful discussions.

References

[1] FUJIWARA, M., et al., Nuclear Fusion **39** (1999) 1659
[2] SANUKI, H., TODOROKI, J., KAMIMURA, T., Phys. Fluids **B2** (1990) 2155. , et al.,
[3] MURAKAMI, S., et al., Nuclear Fusion **34**(1994), 913.
[4] WADE, M.R., THOMAS, T. J., et al., Nuclear Fusion **35**(1995), 1029
[5] HARTMANN, D. A., Plasma Heating and Sustainment in the Ion Cyclotron Range of Grequencies on the Stellarator W7-AS, in Plasma Physics and Controlled Nuclear Fusion Research 1998 (Proc. 17th IAEA Fusion Energy Conf. Yokohama, 1998), Vol. 2 , Vienna (1999), 575
[6] OKADA, H., et al., Nuclear Fusion **36** (1996) 465
[7] OKAMURA, S., et al., in Plasma Physics and Controlled Nuclear Fusion Research 1992 (Proc. 12th IAEA Fusion Energy Conf. Wurzburg, 1992), Vol. 2 , Vienna (1993) 505
[8] ISOBE, M., et al., Review of Scientific Instruments, Vol. **68**, (1997) pp. 532~535.
[9] ISOBE, M., et al., "Experiment on Ripple Induced Losses of Perpendicularly Injected Beam Ions in the Low Aspect Ratio Helical System CHS", submitted to Nuclear Fusion
[10] IIYOSHI, A., et al., Nuclear Fusion **39** (1999), 1063
[11] YAMADA, H., et al., 'Energy Confinement and Thermal Transport Characteristics of Net-Current Free Plasmas in Large Helical Device', in this conference(EXP6/7)
[12] WATARI, T., et al., 'The Performance of ICRF Heated Plasmas in LHD', in this conference(EXP8/4)
[13] SAITO, K., et al., "Ion Heating and Electron Heating in ICRF Heating Experiment on LHD", submitted to Nuclear Fusion
[14] MUTOH, T., et al., "Ion Heating and High-Energy-Particle Production by Ion Cyclotron Range of Frequencies Heating in the Large Helical Device", submitted to Phys. Rev. Lett.
[15] KRASILNIKOV, A. V., et al. J. of Plasma and Fusion Research, Vol. **75** (1999) 967
[16] ISOBE, M. et al, to be published in Rev. Sci. Instrum.
[17] MURAKAMI., S., et al., Nuclear Fusion **40** (2000) 693.
[18] MURAKAMI., S., et al., Trans. Fusion Technology **27** (1995) 256.

Recent Issues of NIFS Series

NIFS-618 M M Skoric, T Sato, A Maluckov and M S Jovanovic,
Complexity in Laser Plasma Instabilities Dec 1999

NIFS-619 T-H Watanabe, H Sugama and T Sato,
Non-dissipative Kinetic Simulation and Analytical Solution of Three-mode Equations of Ion Temperature Gradient Instability, Dec 1999

NIFS-620 Y Oka, Y Takeiri, Yu.I Belchenko, M Hamabe O Kaneko, K. Tsumori, M Osakabe, E Asano, T. Kawamoto, R. Akiyama,
Optimization of Cs Deposition in the 1/3 Scale Hydrogen Negative Ion Source for LHD-NBI System ,Dec 1999

NIFS-621 Yu I Belchenko, Y. Oka, O Kaneko, Y Takeiri, A Krivenko, M Osakabe, K Tsumori, E Asano, T Kawamoto, R Akiyama,
Recovery of Cesium in the Hydrogen Negative Ion Sources,Dec. 1999

NIFS-622 Y. Oka, O. Kaneko, K Tsumori, Y Takeiri, M Osakabe, T. Kawamoto, E Asano, and R. Akiyama,
H- Ion Source Using a Localized Virtual Magnetic Filter in the Plasma Electrode: Type I LV Magnetic Filter: Dec 1999

NIFS-623 M Tanaka, S Kida, S. Yanase and G. Kawahara,
Zero-absolute-vorticity State in a Rotating Turbulent Shear Flow,Jan 2000

NIFS-624 F Leuterer, S Kubo,
Electron Cyclotron Current Drive at $\omega \approx \omega_c$ with X-mode Launched from the Low Field Side; Feb. 2000

NIFS-625 K Nishimura,
Wakefield of a Charged Particulate Influenced by Emission Process of Secondary Electrons; Mar 2000

NIFS-626 K Itoh, M. Yagi, S-I Itoh, A Fukuyama,
On Turbulent Transport in Burning Plasmas;Mar. 2000

NIFS-627 K Itoh, S-I. Itoh, L. Giannone,
Modelling of Density Limit Phenomena in Toroidal Helical Plasmas; Mar. 2000

NIFS-628 K Akaishi, M Nakasuga and Y. Funato,
True and Measured Outgassing Rates of a Vacuum Chamber with a Reversibly Absorbed Phase;Mar. 2000

NIFS-629 T Yamagishi,
Effect of Weak Dissipation on a Drift Orbit Mapping, Mar 2000

NIFS-630 S Toda, S -I, itoh, M Yagi, A Fukuyama and K Itoh,
Spatial Structure of Compound Dither in L/H Transition,Mar. 2000

NIFS-631 N Ishihara and S Kida,
Axial and Equatorial Magnetic Dipoles Generated in a Rotating Spherical Shell; Mar 2000

NIFS-632 T Kuroda, H Sugama, R Kanno and M. Okamoto,
Ion Temperature Gradient Modes in Toroidal Helical Systems, Apr. 2000

NIFS-633 V.D Pustovitov,
Magnetic Diagnostics: General Principles and the Problem of Reconstruction of Plasma Current and Pressure Profiles in Toroidal Systems, Apr 2000

NIFS-634 A.B. Mikhailovskii, S.V. Konovalov, V.D. Pustovitov and V.S Tsypin,

Mechanism of Viscosity Effect on Magnetic Island Rotation; Apr. 2000

NIFS-635 H. Naitou, T. Kuramoto, T. Kobayashi, M. Yagi, S. Tokuda and T. Matsumoto,
Stabilization of Kinetic Internal Kink Mode by Ion Diamagnetic Effects; Apr. 2000

NIFS-636 A. Kageyama and S. Kida,
A Spectral Method in Spherical Coordinates with Coordinate Singularity at the Origin; Apr. 2000

NIFS-637 R. Horiuchi, W. Pei and T. Sato,
Collisionless Driven Reconnection in an Open System; June 2000

NIFS-638 K. Nagaoka, A. Okamoto, S. Yoshimura and M.Y. Tanaka,
Plasma Flow Measurement Using Directional Langmuir Probe under Weakly Ion-Magnetized Conditions; July 2000

NIFS-639 Alexei Ivanov,
Scaling of the Distribution Function and the Critical Exponents near the Point of a Marginal Stability under the Vlasov-Poisson Equations; Aug. 2000

NIFS-640 K. Ohi, H. Naitou, Y. Tauchi, O. Fukumasa,
Observation of the Limit Cycle in the Asymmetric Plasma Divided by the Magnetic Filter; Aug. 2000

NIFS-641 H. Momota, G.H. Miley and J. Nadler,
Direct Energy Conversion for IEC Propulsions; Aug 2000

NIFS-642 Y. Kondoh, T. Takahashi and H. Momota,
Revisit to the Helicity and the Generalized Self-organization Theory; Sep. 2000

NIFS-643 H. Soltwisch, K. Tanaka,
Changes of the Electron Density Distribution during MHD Activity in CHS: Sep. 2000

NIFS-644 Fujisawa, A., Iguchi, H., Minami, T., Yoshimura, Y., Sanuki, H., Itoh, K., Isobe, M., Nishimura, S., Tanaka, K., Osakabe, M., Nomura, I., Ida, K., Okamura, S., Toi, K., Kado, S., Akiyama, R., Shimizu, A., Takahashi, C., Kojima, M., Matsuoka, K., Hamada, Y., Fujiwara, M.,
Observation of Bifucation Property of Radial Electric Field Using a Heavy Ion Beam Probe: Sep. 2000
(IAEA-CN-77/EX6/6)

NIFS-645 Todo, Y., Watanabe, T.-H., Park, H.-B., Sato, T.,
Fokker-Planck Simulation Study of Alfvén Eigenmode Burst Sep. 2000
(IAEA-CN-77/TH6/2)

NIFS-646 Muroga, T., Nagasaka, T.,
Development of Manufacturing Technology for High Purity Low Activation Vanadium Alloys: Sep. 2000
(IAEA-CN-77/FTP1/09)

NIFS-647 Itoh, K., Sanuki, H., Toda, S., Itoh, S.-I., Yagi, M., Fukuyama, A., Yokoyama, M.,
Theory of Dynamics in Long Pulse Helical Plasmas: Sep. 2000
(IAEA-CN-77/THP1/19)

NIFS-648 R. Sakamoto, H. Yamada, K. Tanaka, K. Narihara, S. Morita, S. Sakakibara, S. Masuzaki, L.R. Baylor, P.W. Fisher, S.K. Combs, M.J. Gouge, S. Kato, A. Komori, O. Kaneko, N. Ashikawa, P. de Varies, M. Emoto, H. Funaba, M. Goto, K. Ida, H. Idei, K. Ikeda, S. Inagaki, M. Isobe, S. Kado, K. Kawahata, K. Khlopenkov, S. Kubo, R. Kumazawa, T. Minami, J. Miyazawa, T. Morisaki, S. Murakami, S. Muto, T. Mutoh, Y. Nagayama, Y. Nakamura, H. Nakanishi, K. Nishimura, N. Noda, T. Notake, T. Kobuchi, Y. Liang, S. Ohdachi, N. Ohyabu, Y. Oka, M. Osakabe, T. Ozaki, R.O. Pavlichenko, B.J. Peterson, A.

Sagara, K. Saito, H. Sasao, M. Sasao, K Sato, M. Sato, T Seki, T Shimozuma, M. Shoji, S Sudo, H. Suzuki, M. Takechi, Y. Takeiri, N. Tamura, K Toi, T. Tokuzawa, Y Torii, K Tsumori, I Yamada, S. Yamaguchi, S. Yamamoto, Y Yoshimura, K Y Watanabe, T Watari, K Yamazaki, Y Hamada, O Motojima and M Fujiwara,

Impact of Pellet Injection on Extension of Operational Region in LHD: Sep 2000
(IAEA-CN-77/ EXP4/18)/

NIFS-649 K Ichiguchi, M. Wakatani, T Unemura, T Tatsuno and B.A. Carreras

Improved Stability due to Local Pressure Flattening in Stellarators: Sep 2000
(IAEA-CN-77/ THP2/08)

NIFS-650 N Noda, Y. Nakamura, Y. Takeiri, T. Mutoh, R. Kumazawa, M Sato, K Kawahata, S. Yamada, T. Shimozuma, Y. Oka, A. Iiyoshi , R Sakamoto, Y. Kubota, S. Masuzaki, S. Inagaki, T. Morisaki, H. Suzuki, N. Ohyabu, K. Adachi, K. Akaishi, N. Ashikawa, H. Chikaraishi, P. C. de Vries , M Emoto, H. Funaba, M. Goto, S. Hamaguchi, K. Ida, H. Idei, K. Ikeda, Imagawa, N. Inoue, M. Isobe, A. Iwamoto, S. Kado , O. Kaneko, S. Kitagawa, K Khlopenkov, T. Kobuchi, A Komori, S. Kubo, Y. Liang, R. Maekawa, T Minami, T. Mito, J. Miyazawa, S Morita, K. Murai, S. Murakami, S Muto, Y. Nagayama, H. Nakanishi, K. Narihara, A. Nishimura, K. Nishimura, A Nishizawa, T. Notake, S. Ohdachi, M. Okamoto, M. Osakabe, T. Ozaki, R. O. Pavlichenko, B. J. Peterson, A. Sagara, K. Saito, S. Sakakibara, H. Sasao, M. Sasao, K. Sato, T. Seki, M. Shoji, H Sugama, K. Takahata, M. Takechi, H. Tamura, N. Tamura, K. Tanaka, K. Toi, T. Tokuzawa, Y. Torii, K. Tsumori, K. Y. Watanabe, T. Watanabe, T. Watari, N. Yanagi, I. Yamada, H. Yamada, S. Yamaguchi, S. Yamamoto, T. Yamamoto, M. Yokoyama, Y. Yoshimura, I. Ohtake, R. Akiyama, K. Haba, M. Iima, J. Kodaira, K Tsuzuki, K. Itoh, K Matsuoka, K. Ohkubo, S. Satoh, T. Satow, S. Sudo, S. Tanahashi, K. Yamazaki, O. Motojima, Y. Hamada, M. Fujiwara,

Experimental Studies toward Long-Pulse Steady-State Operations in LHD: Sep 2000
(IAEA-CN-77/ EX4/5)

NIFS-651 H.Yamada, K.Y.Watanabe, K.Yamazaki, S.Murakami, S.Sakakibara, K.Narihara, K.Tanaka, M.Osakabe, K.Ida, G.Rewoldt, N.Ashikawa, P.deVaries, M.Emoto, H.Funaba, M.Goto, H.Idei, K.Ikeda, S. Inagaki, N.Inoue, M.Isobe, S.Kado, O.Kaneko, K.Kawahata, K.Khlopenkov, A.Komori, S.Kubo, R.Kumazawa, S.Masuzaki, T.Minami, J.Miyazaw a, T.Morisaki, S.Morita, S.Muto, T.Mutoh, Y Nagayama, N.Nakajima, Y.Nakamura, H.Nakanishi, K.Nishimura, N.Noda, T Notake, T.Kob uchi, Y.Liang, S.Ohdachi, N.Ohyabu, Y.Oka, T.Ozaki, R.O.Pavlichenko, B.J.Peterson, A.Sagara, K.Saito, R.Sakamoto, H.Sasao, M.Sasao, K.Sato, M.Sato, T Seki, T.Shimozuma, M Shoji, H.Sugama, H.Suzuki, M.Takechi, Y.Takeiri, N.Tamura, K.Toi, T.Tokuzawa, Y.Torii, K.Tsumori, I.Yamada, S.Yamaguchi, S.Yamamoto, M.Yokoyama, Y.Yoshimura, T.Watari, K Itoh, K.Matsuoka, K Ohkubo, I.Ohtake, S.Satoh, T.Satow, S.Sudo, S.Tanahashi, T.Uda, Y.Hamada, O.Motojima, M.Fujiwara,

Energy Confinement and Thermal Transport Characteristics of Net-Current Free Plasmas in Large Helical Device: Sep 2000
(IAEA-CN-77/ EX6/7)

NIFS-652 S. Sakibara, H. Yamada, K. Y. Watanabe, Y Narushima, K. Toi, S Ohdachi, M. Takichi, S. Yamamoto, K. Narihara, K. Tanaka, N. Ashikawa, P. Devaries, M. Emoto, H. Funaba, M. Goto, K. Ida, H. Idei, K. Ikeda, S. Inagaki, N. Inoue, M. Isobe, S. Kado, O. Kaneko, K. Kawahata, K. Khlopenkov, A. Komori, S. Kubo, R. Kumazawa,S. Masuzaki, T. Minami, J. Miyazawa, T. Morisaki, S Morita, S. Murakami, S. Muto, T. Mutoh, Y. Nagayama, Y. Nakamura, H. Nakanishi, K. Nishimura, N. Noda, T. Notake, T. Kobuchi, Y. Liang, N. Ohyabu, Y. Oka, M. Osakabe, T. Ozaki, R.O. Pavlichenko, B.J. Peterson, A. Sagara, K Saito, R Sakamoto, H. Sasao, M. Sasao, K. Sato, M. Sato, T. Seki, T. Shimozuma, M. Shoji, H. Suzuki, Y. Takeiri, N. Tamura, T. Tokuzawa, Y. Torii, K. Tsumori, I. Yamada, S. Yamaguchi, M. Yokoyama, Y. Yoshimura, T. Watari,N. Nakajima, K. Ichiguchi, H. Takahashi, A.W. Cooper, K Yamazaki, O. Motojima, Y. Hamada, M. Fujiwara

MHD Characteristics in High-β Regime of the Large Helical Device: Sep 2000
(IAEA-CN-77/ EXP3/12)

NIFS-653 M. Fujiwara, K. Kawahata, N. Ohyabu, O. Kaneko, A Komori, H. Yamada, N Ashikawa, L.R. Baylor, S.K. Combs, P.C. deVries, M. Emoto, A. Ejiri, P.W. Fisher, H. Funaba, M. Goto, D. Hartmann, K. Ida, H. Idei, S. Iio, K. Ikeda, S. Inagaki, N. Inoue, M. Isobe, S Kado, K. Khlopenkov, T. Kobuchi, A.V. Krasilnikov, S. Kubo, R Kumazawa, F. Leuterer, Y. Liang, J F. Lyon, S Masuzaki, T. Minami, J. Miyajima, T. Morisaki, S. Morita, S. Murakami, S.Muto T. Mutoh, Y. Nagayama, N. Nakajima, Y.

Nakamura, H. Nakanishi, K. Narihara, K. Nishimura, N. Noda, T. Notake, S. Ohdachi, Y. Oka, S. Okajima, M. Okamoto, M. Osakabe, T. Ozaki, R.O. Pavlichenko, B.J. Peterson, A. Sagara, K. Saito, S. Sakakibara, R. Sakamoto, H. Sanuki, H. Sasao, M. Sasao, K. Sato, M. Sato, T. Seki, T. Shimozuma, M. Shoji, H. Sugama, H. Suzuki, M. Takechi, Y. Takeiri, N.Tamura, K. Tanaka, K. Toi, T. Tokuzawa, Y. Torii, K.Tsumori, K. Y. Watanabe, T. Watanabe, T. Wateri, I. Yamada, S. Yamaguchi, S. Yamamoto, M. Yokoyama, N. Yoshida, Y. Yoshimura, Y. P. Zhao, R. Akiyama, K. Haba, M. Iima, J. Kodaira, T. Takita, T. Tsuzuki, K. Yamauchi, H. Yonezu, H. Chikaraishi, S. Hamaguchi, S. Imagawa, N. Inoue, A. Iwamoto, S. Kitagawa, Y. Kubota, R. Maekawa, T. Mito, K. Murai, A. Nishimura, H. Chikaraishi, K. Takahata, H. Tamura, S. Yamada, N. Yanagi, K. Itoh, K. Matsuoka, K. Ohkubo, I. Ohtake, S. Satoh, T. Satow, S. Sudo, S. Tanahashi, K. Yamazaki, Y. Hamada, O. Motojima,

Overview of LHD Experiments: Sep. 2000
(IAEA-CN-77/OV1/4)

NIFS-654 S. Okamura, K. Matsuoka, S. Nishimura, M. Isobe, I. Nomura, C. Suzuki, A. Shimizu, S. Murakami, N. Nakajima, M Yokoyama, A. Fujisawa, K. Ida, K. Itoh, P. Merkel, M. Drevlak, R. Zille, S. Gori, J. Nührenberg,

Physics and Engineering Design of a Low-Aspect-Ratio Quasi-Axisymmetric Stellarator CHS-qa: Sep. 2000
(IAEA-CN-77/ICP/16)

NIFS-655 K.Ida, H.Funaba, S.Kado , K.Narihara, K.Tanaka, Y.Takeiri, Y.Nakamura, N.Ohyabu, K.Yamazaki, M.Yokoyama, S.Murakami, N.Ashikawa, P.deVaries, M.Emoto, M.Goto, H.Idei, K.Ikeda, S.Inagaki, N.Inoue, M.Isobe, K.Itoh, O.Kaneko, K.Kawahata, K.Khlopenkov, A.Komori, S.Kubo, R.Kumazawa, Y.Liang , S.Masuzaki, T.Minami, J.Miyazawa, T.Morisaki, S.Morita, T.Mutoh, S.Muto, Y.Nagayama, H.Nakanishi, K.Nishimura, N.Noda, T.Notake , T.Kobuchi, S.Ohdachi, K.Ohkubo, Y.Oka, M.Osakabe, T.Ozaki, R.O.Pavlichenko, B.J. Peterson, A.Sagara, K.Saito , S.Sakakibara, R.Sakamoto, H.Sanuki, H.Sasao, M.Sasao, K.Sato, M.Sato, T.Seki, T. Shimozuma, M.Shoji, H.Suzuki, S.Sudo, N.Tamura , K. Toi, T. Tokuzawa, Y.Torii , K.Tsumori, T.Yamamoto, H.Yamada, I.Yamada, S.Yamaguchi, S.Yamamoto , Y.Yoshimura, K.Y.Watanabe, T.Watari, Y.Hamada, O.Motojima, M.Fujiwara,

Transition From Ion Root to Electron Root in NBI Heated Plasmas in LHD: Sep. 2000
(IAEA-CN-77/EX9/4)

NIFS-656 K.Narihara, I.Yamada, N.Ohyabu, K.Y.Watanabe, N.Ashikawa, P.C.deVries, M. Emoto, H.Funaba, M.Goto, K.Ichiguchi, K.Ida, H.Idei, K.Ikeda, S.Inagaki, N.Inoue, K.Isobe, S.Kado, O.Kanako, K.Kawahata, K. Khlopenkov, T.Kobuchi, A.Komori, S.Kubo, R.Kumazawa, Y.Liang, T.Masuzaki, T.Minami, J.Miyazawa, T.Morisaki, S.Morita, S.Murakami, S.Muto, T.Mutoh, Y.Nagayama, Y.Nakamura, H.Nakanishi, Y.Narushima, K.Nishimura, N.Noda, T.Notake, S.Ohdachi, Y.Oka, M.Osakabe, S.Ozaki, R.O.Pavlichenko, B.J.Peterson, A.Sagara, K.Saito, S.Sakakibara, R.Sakamoto, H.Sasao, M.Sasao, K.Sato, M.Sato, T.Seki, T.Shimozuma, C.Shoji, H.Suzuki, A.Takayama, M.Takechi, Y.Takeiri, N.Tamura, K.Tanaka, K.Toi, N.Tokuzawa, Y.Torii, K.Tsumori, T.Watari, H.Yamada, S.Yamaguchi, S.Yamamoto, M.Yokoyama, Y.Yoshimura, S.Satow, K.Itoh, K.Ohkubo, K.Yamazaki, S.Sudo, O.Motojima, Y.Hamada, M.Fujiwara,

Transition from Ion Root to Electron Root in NBI Heated Plasmas in LHD: Sep. 2000
(IAEA-CN-77/EXP5/28)

NIFS-657 M. Sasao, S. Murakami, M. Isobe, A.V. Krasilnikov, S. Iiduka, K. Itoh, N. Nakajima, M. Osakabe, K.Saito,T. Seki, Y.Takeiri, T. Watari, N.Ashikawa , P.deVaries, M.Emoto, H.Funaba, M.Goto, K.Ida, H.Idei, K.Ikeda, S.Inagaki, N.Inoue, S.Kado, O.Kaneko, K.Kawahata, K.Khlopenkov, T.Kobuchi , A.Komori, S.Kubo, R.Kumazawa, S.Masuzaki, T.Minami, J.Miyazawa, T.Morisaki, S.Morita, S.Muto, T.Mutoh, Y.Nagayama, Y.Nakamura, H.Nakanishi, K.Narihara, K.Nishimura, N.Noda, T.Notake, Y.Liang , S.Ohdachi, N.Ohyabu, Y.Oka, T.Ozaki, R.O.Pavlichenko, B.J.Peterson, A.Sagara, S.Sakakibara, R.Sakamoto, H.Sasao4, K.Sato, M.Sato, T.Shimozuma, M.Shoji, H.Suzuki, M.Takechi, N.Tamura, K.Tanaka, K.Toi, T.Tokuzawa, Y.Torii, K.Tsumori, H.Yamada, I.Yamada, S.Yamaguchi, S.Yamamoto, M.Yokoyama, Y.Yoshimura, K.Y.Watanabe and O. Motojima,

Study of Energetic Ion Transport in the Large Helical Device: Sep. 2000
(IAEA-CN-77/EX9/1)